International Journal of Nanomedicine

Dovepress
open access to scientific and medical research

Open Access Full Text Article

ORIGINAL RESEARCH

Intratracheal instillation of ethyl pyruvate nanoparticles prevents the development of shunt-flow-induced pulmonary arterial hypertension in a rat model

This article was published in the following Dove Press journal:
International Journal of Nanomedicine
3 June 2016
Number of times this article has been viewed

Kai Liu[1]
Xiquan Zhang[1]
Guangqing Cao[1]
Yongjun Liu[2]
Chuanzhen Liu[1]
Hourong Sun[1]
Xinyan Pang[1]

[1]Cardiovascular Surgery Department, Qilu Hospital of Shandong University, [2]Pharmacy College of Shandong University, Jinan, People's Republic of China

Purpose: To investigate whether inhalation of ethyl pyruvate (EP) encapsulated with poly(ethylene glycol)-*block*-lactide/glycolide copolymer nanoparticles (EP-NPs) can prevent the development of shunt-flow-induced hyperkinetic pulmonary arterial hypertension (PAH) in a rat model.

Materials and methods: Rats were separated into five groups: blank (ie, no treatment after shunt flow), normal control (ie, no shunt flow or treatment), EP-NP instillation, EP-only instillation, and vehicle. The animals received intratracheal instillation of EP-NPs or other treatments immediately after a shunt flow, and treatment continued weekly until the end of the experiment. Hemodynamic data were recorded, pulmonary arterial remodeling was assessed, and levels of inflammatory mediators and ET1 expression in the lung and serum were analyzed. In addition, retention of EP in the lungs of rats in the EP-NP and EP-only groups was measured using high-performance liquid chromatography.

Results: After 12 weeks, hemodynamic abnormalities and pulmonary arterial remodeling were improved in the EP-NP instillation group, compared with the blank, EP-only, and vehicle groups ($P<0.05$). In addition, the EP-NP group showed significantly decreased levels of HMGB1, IL-6, TNFα, reactive oxygen species, and ET1 in the lung during PAH development ($P<0.05$). Furthermore, EP-NP instillation was associated with reduced serum levels of inflammatory factors and ET1. High-performance liquid-chromatography measurement indicated that EP retention was greater in the lungs of the EP-NP group than in the EP-only group.

Conclusion: EP-NP instillation attenuated inflammation and prevented pulmonary arterial remodeling during the development of PAH induced by shunt flow. In the future, EP-NP delivery into the lung might provide a novel approach for preventing PAH.

Keywords: pulmonary artery hypertension, ethyl pyruvate, high-mobility group box 1

Introduction

Pulmonary arterial hypertension (PAH) is generally characterized by increased resistance in the pulmonary circulation and occlusive remodeling of the pulmonary arterioles. In addition, elevated afterload of the right ventricle (RV) can result in heart failure and premature death.[1] Left-to-right shunt congenital heart disease exposes the pulmonary vasculature to overflow and high pressure, which leads to endothelial injury and dysfunction, and finally induces hyperkinetic PAH.

Dysfunctional endothelial cells release the nuclear protein HMGB1 and activate proinflammatory cytokines, such as IL-1, IL-6, and TNFα, which themselves

Correspondence: Xinyan Pang
Cardiovascular Surgery Department, Qilu Hospital of Shandong University, 107 Wenhua Xilu, Jinan, Shandong 250012, People's Republic of China
Tel +86 531 8216 6510
Fax +86 531 8216 6581
Email 13793182001@163.com

submit your manuscript | www.dovepress.com
Dovepress
http://dx.doi.org/10.2147/IJN.S103183

enhance the secretion of HMGB1 and further aggravate the inflammatory response to injury. HMGB1 can induce chemotaxis of the smooth-muscle cells, which contributes to the formation of intimal hypertrophy.[2] Studies have also shown that HMGB1 promotes the development of PAH.[3,4]

It is known that inflammation plays a pivotal role in disease progression in various types of PAH.[5–8] Inflammatory factors participate in vasoconstriction, promote hyperplasia of pulmonary vascular endothelial cells and smooth-muscle cells, and subsequently result in remodeling of the pulmonary vasculature.[9] In addition to an increase in inflammatory mediators, endothelial cell injury caused by increased blood flow also leads to mitochondrial dysfunction, which is the major source of reactive oxygen species (ROS) production in PAH. ROS derived from mitochondria induce pulmonary vascular remodeling by increasing intracellular Ca^{2+}, depolarization/hyperpolarization of the mitochondrial membrane potential ($\Delta\Psi_m$), and smooth-muscle cell contraction and proliferation.[10,11] Therefore, HMGB1 and ROS play a central role in tissue remodeling and angiogenesis, and both are crucial in the pathogenesis of PAH.[12]

Targeting a battery of multiple important inflammatory cytokines might be a favorable therapeutic approach for PAH. Ethyl pyruvate (EP), which is a simple derivative of pyruvic acid, is an ROS scavenger, inflammatory suppressor, and HMGB1 inhibitor. Treatment with EP has been shown to improve survival or ameliorate organ dysfunction in a wide variety of preclinical models, including models of severe sepsis, acute lung injury, and acute pancreatitis.[13–15] Considering the pathophysiology of PAH and the roles of HMGB1 and ROS in the progression of this disease, it is reasonable to hypothesize that inhibition of HMGB1 and ROS might prevent the development of PAH. Indeed, our previous study showed that intraperitoneal injection of EP could attenuate monocrotaline-induced PAH and reverse pulmonary vascular remodeling in rats by inhibiting the release of TNFα and IL-6 and reducing the expression of ET1.[16]

Nebulized inhalation appears to be more efficient than systemic drug delivery of targeted therapy in pulmonary disease. Compared with systemic administration, local delivery of a drug would be expected to increase its distribution in the lungs, improve the efficiency of the targeted therapy, eliminate side effects, and avoid first-pass elimination by the liver. Because EP is a volatile substance that is unstable at normal temperatures, it must be pretreated in order to achieve long-term efficiency. Moreover, EP pretreatment with a biocompatible and biodegradable polymer might enable prolonged efficiency and decreased administration frequency. Therefore, we developed bioabsorbable polymeric nanoparticles (NPs) formulated from a poly(ethylene glycol)-*block*-lactide/glycolide copolymer (PEG-LG). We hypothesized that pulmonary administration of EP encapsulated in PEG-LG NPs (EP-NPs) would provide superior protective effects in comparison with free EP during the development of hyperkinetic PAH by suppressing proinflammatory factors.

Materials and methods

Preparation of EP-NPs and characterizations

The amphiphilic block copolymer PEG-LG (molecular weight 30,000, 7% PEG, ratio of lactide to glycolide 75:25; Jinan Daigang Biomaterial Co Ltd, Jinan, People's Republic of China [PRC]) was used as the drug carrier. EP-NPs (EP from Sigma-Aldrich, St Louis, MO, USA) was prepared using an emulsion solvent-evaporation method, as reported previously.[17,18] Fluorescein isothiocyanate (FITC) solution and EP-NPs were dissolved in dichloromethane to form a water-in-oil emulsion after high-speed shearing. The compound was added dropwise into a 3% polyvinyl alcohol solution with slow stirring, and the dichloromethane was volatilized to form a water-in-oil-in-water emulsion. After three rounds of centrifugation, washing, and vacuum-drying, EP-FITC-NPs were obtained. The formulation showed a smooth appearance and well-distributed particles under transmission electron microscopy (Figure 1A). The encapsulation efficiency and loading capacity of EP-FITC-NPs, as measured by high-performance liquid chromatography (HPLC), were 85.84%±6.08% and 8.82%±0.81%, respectively. A sample of EP-FITC-NP suspension in distilled water was used for particle-size analysis. The average diameter of the formulation was 286.04±35.11 nm (Figure 1B), and the polydispersion index was 0.131±0.016. The experimental aerodynamic diameter of the formulation was 2.1 μm, which was within the range of the optimal size for inhalation (0.5–5 μm). The surface charge (ζ-potential) was −15.21±2.57 mV, which was analyzed using the Zetasizer 3000 (Malvern Instruments, Malvern, UK) (Figure 1C). All measurements were carried out in triplicate. The values reported are mean ± standard deviation (n=3).

Experimental animal models and group definition

The study protocols were approved by the Ethical and Legal Committee of the National Institutes of the Care and Use of Laboratory Animals. All animals received humane care and the experiments were performed in accordance with the guidelines of the Animal Care and Use Committee of Shandong University. Hyperkinetic PAH was established

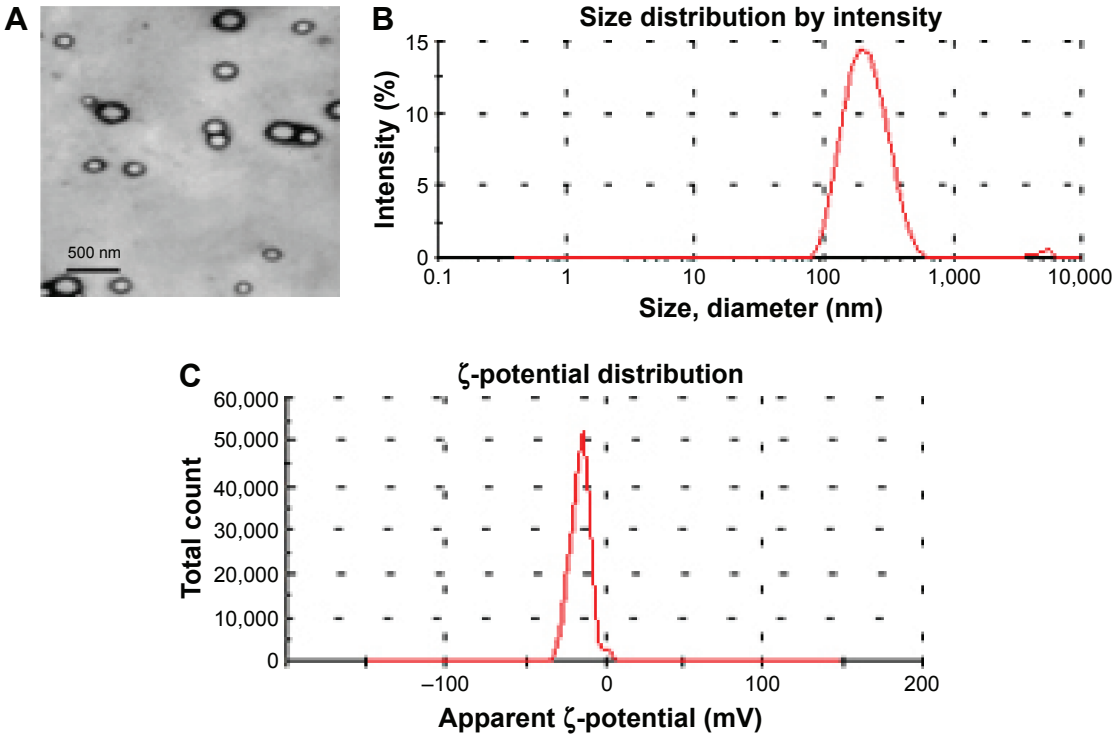

Figure 1 Characterization of EP-NPs.
Notes: (**A**) Appearance of EP-NPs under transmission electron microscopy; (**B**) diameter data of EP-NP formulation; (**C**) ζ-potential of EP-NPs. All measurements were carried out in triplicate.
Abbreviation: EP-NPs, ethyl pyruvate nanoparticles.

in male Sprague Dawley rats (120–150 g body weight; from the Animals Experimental Center of Shandong University) by shunt flow, according to a previously described method in which PAH was induced after 12 weeks.[19]

The animals were divided into five groups: blank (no treatment after shunt flow), normal control (no shunt flow and no treatment), EP-NPs (1 mg EP per 12 mg FITC-PEG-LG in 0.2 mL phosphate-buffered saline [PBS] for instillation), EP only (1 mg EP in 0.2 mL PBS for instillation), and vehicle (12 mg FITC-PEG-LG in 0.2 mL PBS for instillation). The animals received intratracheal instillation immediately after a shunt flow was performed, and the treatment was repeated each week thereafter until the end of the experiment. In brief, a 0.2 mL suspension of EP-NPs, EP alone, or vehicle alone was gently instilled into the trachea. Immediately before instillation, circumferential compression of the thorax was performed to achieve forced exhalation. The compression was released after endotracheal instillation followed by 5 mL air. This caused a forceful inspiration that facilitated access of the drug to the distal air spaces. The inhalational dose of EP-NPs was selected after we examined the effects of intratracheal instillation of various concentrations and volumes of EP-NP suspension (0.5, 1, 2, and 4 mg per animal in 0.1, 0.2, 0.4, and 0.8 mL PBS) on the basis of the largest improvement in the model, with the fewest complications and side effects. We confirmed that a 0.2 mL suspension containing 1 mg EP was the optimal dose for our experiments.

Biodistribution of FITC-NP examination

Rats received instillation of FITC, FITC-NP, and NPs alone. Localization of FITC in the lung was observed 24 hours later. The animals were killed, and the lungs were washed with PBS using a catheter inserted into the trachea, resected, and then inflated with 10% phosphate-buffered formalin (pH 7.4). Tissues were embedded in tissue-freezing medium (OCT compound; Sakura Finetek, Tokyo, Japan), and cross sections of 3 μm thickness were prepared. The sections were first incubated with Sky Blue to eliminate nonspecific fluorescence, and FITC-NP distribution was then observed under a fluorescence microscope. Fluorescence intensity was also observed at 1, 3, and 7 days after a single intratracheal instillation of FITC-NPs into rats that had undergone shunt flow, in order to assess FITC retention.

Measurement of hemodynamic parameters

Hemodynamic parameters were measured 12 weeks after the first treatment. The rats were anesthetized with an intraperitoneal injection of 0.25% pentobarbital sodium

(40 mg/kg), intubated, and supported with a ventilator. Pulmonary arterial pressure (PAP) and systemic pressure were measured as described previously.[15] In brief, two catheters were inserted into the main pulmonary artery and the right common carotid artery under fluoroscopic guidance to measure PAP (including diastolic PAP, systolic PAP, and mean PAP) and mean systemic arterial pressure, respectively. The two catheters were linked to a transducer, and the pressure was simultaneously recorded on a multichannel physiologic recorder (PowerLab 8/30; AD Instruments Pty Ltd, Sydney, Australia). Each measurement was read three times, and the mean value was used in the final results.

Preparation of heart and lung tissues

After hemodynamic measurement, the rats were killed with an overdose of pentobarbital sodium. The lungs were washed in PBS, the lower lobe was removed to measure EP retention, and a part of the lower lobe was placed into liquid nitrogen for other experiments. The remainder of the lungs was immersed into 10% phosphate-buffered formalin and embedded in paraffin according to standard procedures, and 5 μm sections were prepared for further morphologic analysis and immunostaining. The heart was weighed after the liquid was blotted for comparison of the weight ratio of heart to body. The heart was then separated into the RV and the left ventricle plus ventricular septum (LV+VS), and the ratio of the weight of the RV to that of the LV+VS was calculated to evaluate RV hypertrophy.

Enzyme-linked immunosorbent assay

At the end of catheterization, blood was collected, transferred into tubes, and stored on ice. Serum was separated by centrifugation at 4°C and then stored at −80°C for further analysis. The levels of IL-6, TNFα, ET1, and HMGB1 were determined by enzyme-linked immunosorbent assay (ELISA) according to the manufacturer's protocols (IL-6, TNFα, and ET1 kits were from BD [Franklin Lakes, NJ, USA], and the HMGB1 kit was from Shino-Test Corporation [Tokyo, Japan]).

Morphologic and immunohistochemistry analysis

Slices were stained with hematoxylin–eosin, and the small arteries (external diameter 50–200 μm, selected randomly under a low-power field) in the lung were observed under an optical microscope (BX51; Olympus, Tokyo, Japan). External and internal diameters were measured by a blinded observer. The medial wall thickness and medial wall area were calculated as described previously, and represented remodeling of the vessels.[20,21] The medial wall thickness index (TI) and area index (AI) were calculated as follows:

$$\text{TI}\,(\%) = \frac{\text{External diameter} - \text{Internal diameter}}{\text{External diameter}} \times 100 \quad (1)$$

$$\text{AI}\,(\%) = \frac{\text{Total area} - \text{Internal area}}{\text{Total area}} \times 100 \quad (2)$$

For immunohistochemistry, each slice was treated with hydrogen peroxide, blocked with 5% bovine serum albumin, and successively incubated with primary antibodies (goat anti-IL-6, goat anti-TNFα; both from Santa Cruz Biotechnology Inc, Dallas, TX, USA) overnight at 48°C. After the uncombined primary antibody was washed, the slice was incubated with horseradish peroxidase-coupled secondary antibody for 30 minutes at 37°C. The primary antibody was substituted with PBS for a negative control. Peroxidase activity was visualized by a color reaction with diaminobenzidine, with a positive result represented by a brown color. The slices were counterstained with hematoxylin and mounted. Protein levels were quantified using the Image-Pro Plus 6.0 system. The pathologist reviewing the sections was blinded to the experimental groups.

Western blot

Protein was drawn from 20 mg lung tissue on ice by treatment with lysis buffer and phenylmethanesulfonyl fluoride (both from Beyotime, Shanghai, PRC). Protein supernatants were centrifuged at 10,000 rpm for 10 minutes (4°C) to remove tissue fragments of the sediments. Protein concentrations were determined using a Bio-Rad protein-assay instrument, and the protein was boiled with loading buffer. Equal amounts of protein from all the lung tissues were dissolved in sodium dodecyl sulfate (SDS) polyacrylamide-gel electrophoresis (PAGE) sample buffer, separated in SDS-PAGE, and transferred onto polyvinylidene fluoride membranes. The membranes were incubated with the respective primary antibodies (rabbit anti-HMGB1 and rabbit anti-ET1; both from Abcam PLC, Cambridge, UK) overnight at 4°C after being blocked with 5% fat-free milk for 2 hours. The blots were incubated with secondary antibodies conjugated to horseradish peroxidase for 1 hour at room temperature with continuous shaking. After washing, the protein blots were detected using an enhanced chemiluminescence kit (EMD Millipore, Billerica, MA, USA) and exposed to X-ray film. Bands were quantified using FluorChem 9900 (ProteinSimple, San Jose, CA, USA), and β-actin was used as an internal reference.

ROS assay

The ROS fluorescence probe dihydroethidium (DHE) was able to penetrate into cells and was oxidized into 2-hydroxyethidium and ethidium, both of which were able to be detected with a fluorescence detector using an emission wavelength of 580 nm and excitation of 480 nm. Fresh tissues embedded in OCT compound were cut into sections of 5 μm thickness and placed on glass slides. The sections were incubated with DHE (5 mM; Vigorous Biotechnology, Beijing, PRC) in a light-protected humidified chamber at 37°C for 30 minutes. Ethidium fluorescence was examined using a fluorescence microscope, and the mean fluorescence expression was calculated as a percentage of the normal control (set to 100%), as described previously.[22,23]

The other sensitive probe for ROS is 2′,7′-dichlorofluorescein diacetate (DCFH-DA), which can be hydrolyzed into DCFH after penetrating cells and the DCFH shows fluorescence under the fluorescence microscope. Tissue expression of ROS was determined using fluorescence emission, as described previously.[24,25] DCFH-DA (Beyotime) in lung-homogenate supernatants was measured using a spectrofluorometer to assess the ROS content. ROS production is presented as fluorescence units per microgram protein.

Another established assay for ROS is malondialdehyde (MDA) measurement. MDA is the production of the lipid peroxidation that is increased under the condition of oxidation stress. The MDA content reflects the ROS level in the tissue. Briefly, lung tissues were ground and the homogenates obtained. After centrifugation (3,500 rpm for 15 minutes), the supernatant was used for the measurement. MDA contents were determined using the assay kits (Jiancheng Bioengineering Co, Jiangsu, PRC) according to the manufacturer's instructions. Then, MDA activity was quantified as absorbance at 532 nm, and the MDA was expressed as nanomoles per milligram protein.

EP-retention measurement

Tissue homogenates were obtained to determine whether EP was retained and to calculate the residual EP content in each organ at the end of the experiment. EP concentrations were measured using a column-switching HPLC method, as described previously.[26] EP levels in the lung at different time points after instillation were also measured. To determine the EP concentration (ng/mL) in plasma, 500 μL plasma mixed with 10% trichloroacetic acid (200 μL) and 1 mL distilled water were centrifuged for 10 minutes at 1,500 rpm, and 500 μL supernatant was analyzed according to the standard curve. The tests were carried out in triplicate, and mean values are shown in the results.

Statistical analysis

Data are shown as mean ± standard deviation. SPSS version 13.0 (SPSS Inc, Chicago, IL, USA) was used for all statistical analyses. One-way analysis of variance with a post hoc test of the least significant difference was used for statistical analysis. A value of $P<0.05$ was considered statistically significant.

Results

Localization of FITC-NPs in the lung after a single instillation

Strong FITC signals were detected on day 1 in rats that received a single intratracheal instillation of FITC-NPs, compared with no fluorescence signals in the lungs of control no-administration rats and of rats administered NPs alone. Only faint FITC signals were observed in the FITC-alone instillation group (Figure 2A). One day after FITC-NP instillation, there were obvious FITC-positive signals in the bronchi, alveoli, alveolar macrophages, and small arteries. Three days after administration, FITC signals remained predominantly in the small arteries and arterioles, as well as in the small bronchi and alveoli in the lungs, albeit with fainter fluorescence compared with the first day. The fluorescence was faint after 7 days, and was mainly retained in the small arteries, arterioles, and alveoli (Figure 2B).

EP-NP inhalation prevented increasing pressure in the pulmonary artery in shunt-flow rats

Analysis of hemodynamic data is shown in Table 1. Compared with the normal group and the EP-NP group, systolic PAP, diastolic PAP, mean PAP, and RV/LV+VS were significantly increased in the blank group, the EP-only group, and the vehicle group (all $P<0.05$). However, there were no significant differences in hemodynamic data between the EP-NP and normal groups. There were no differences in mean systemic arterial pressure among the groups either.

EP-NP instillation inhibited the development of pulmonary arterial remodeling

To determine the effect of EP-NP intratracheal instillation on vascular remodeling, we measured the TI and AI of the lung arterioles (Figure 3). The hematoxylin–eosin stain of the lung tissues showed that the pulmonary small arteries were thickened in the blank, vehicle, and EP-only groups (Figure 3A). In the EP-NP group, the wall of the pulmonary arteriole was slightly thickened. The results indicated that compared with the normal group and the EP-NP group,

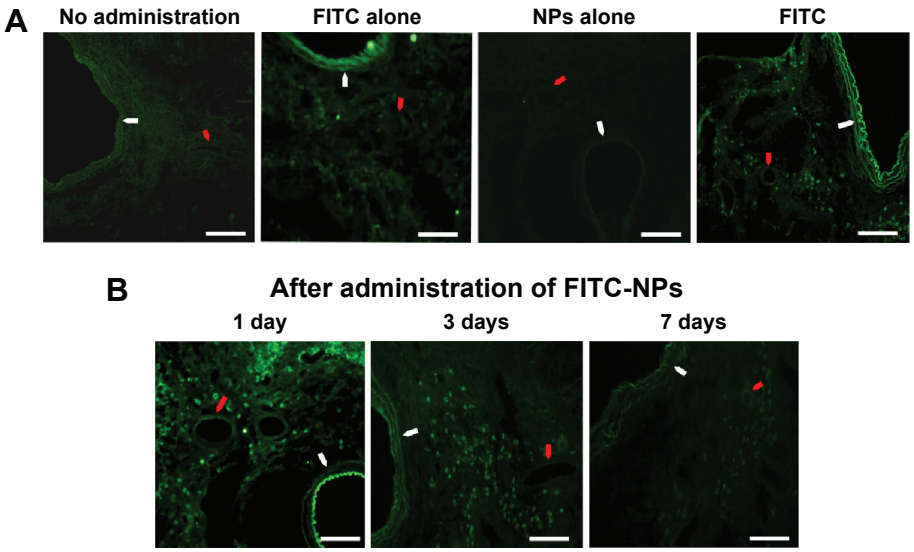

Figure 2 Biodistribution of FITC-NPs in the lung after a single instillation.
Notes: (**A**) Representative fluorescent micrographs of rat lung tissue treated with instillations of FITC-NPs, FITC alone, and NPs alone, and the no-administration group, 1 day after a single instillation. (**B**) Representative fluorescent micrographs of the localization of FITC on days 1, 3, and 7 after a single instillation of FITC-NPs. White arrows indicate bronchia, and red arrows indicate the small arterioles. Scale bars 100 μm.
Abbreviations: FITC-NPs, fluorescein isothiocyanate nanoparticles; FITC, fluorescein isothiocyanate; NPs, nanoparticles.

Table 1 Hemodynamic data of the animals in the different groups

Group	sPAP (mmHg)	dPAP (mmHg)	mPAP (mmHg)	mSAP (mmHg)	Heart/body (g/kg)	RV/LV+VS
Blank	49.8±2.8*,#	23.9±4.7*,#	32.9±2.6*,#	66.6±7.1	3.14±0.12*,#	0.47±0.03*,#
Normal	13.8±2.5	9.1±3.2	11.4±2.8	69.2±4.8	2.51±0.06	0.31±0.02
EP-NPs	17.3±3.8	10.7±1.3	13.8±3.4	67.3±6.3	2.59±0.19	0.34±0.06
EP only	45.4±2.2*,#	21.9±2.9*,#	31.4±2.1*,#	68.9±5.2	2.89±0.11*,#	0.42±0.04*,#
Vehicle	44.7±3.1*,#	22.6±4.5*,#	30.2±3.1*,#	65.8±4.9	2.94±0.08*,#	0.49±0.02*,#

Notes: *$P<0.05$ compared with the normal group; #$P<0.05$ compared with the EP-NP group; n=20 each group. Data shown as mean ± standard deviation.
Abbreviations: PAP, pulmonary arterial pressure; sPAP, systolic PAP; dPAP, diastolic PAP; mPAP, mean PAP; mSAP, mean systemic arterial pressure; LV, left ventricle; RV, right ventricle; VS, ventricular septum; EP-NPs, ethyl pyruvate nanoparticles; EP, ethyl pyruvate.

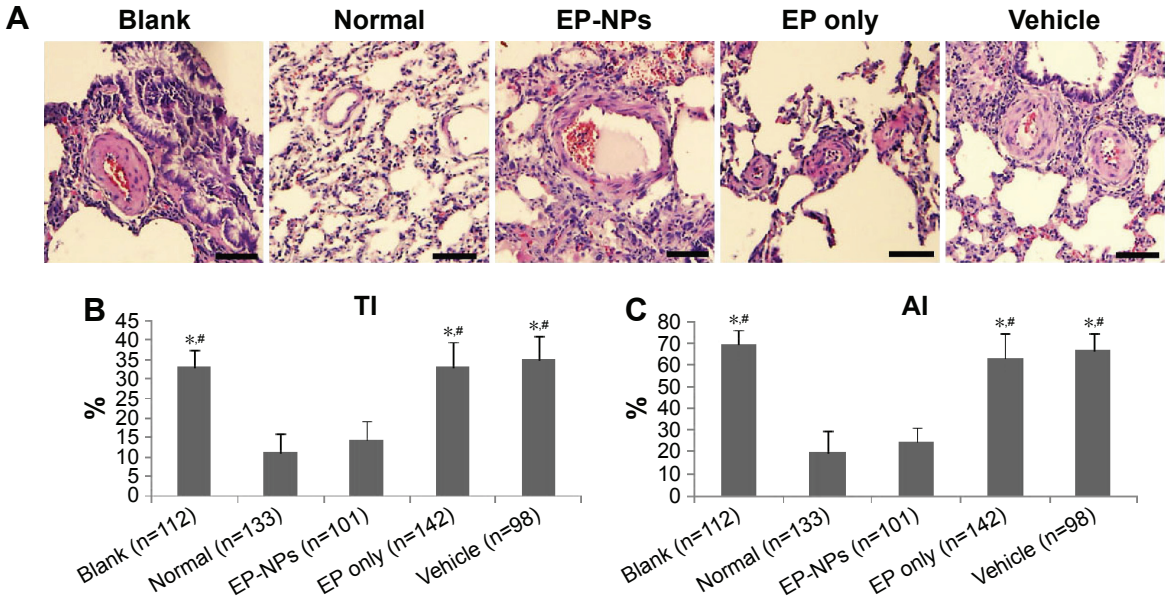

Figure 3 Histopathologic examination of the pulmonary arterioles.
Notes: (**A**) Representative images after hematoxylin–eosin staining. Scale bars 50 μm. (**B**, **C**) Analysis of medial wall thickness index (TI) and medial wall area index (AI) of the small pulmonary arteries in the different groups. Data are mean ± standard deviation (n indicates the number of arteries). *$P<0.05$ versus the normal group; #$P<0.05$ versus the EP-NP group.
Abbreviations: EP-NPs, ethyl pyruvate nanoparticles; EP, ethyl pyruvate.

shunt flow induced a significant increase in the TI and AI of pulmonary arteries in the blank, EP-only instillation, and vehicle groups (all $P<0.05$). There was no statistical difference between the EP-NP and normal control groups in the hypertrophic indices of the arteriole (Figure 3B and C). Therefore, intratracheal instillation with EP-NPs, but not with EP alone or FITC-NP (vehicle), attenuated the development of PAH and small pulmonary arterial remodeling.

EP-NP instillation reduced the expression of proinflammatory factors and ET1 in lung tissues

As shown in Figure 4A, there were a lot of positive signals for IL-6 and TNFα in the blank, EP-only, and vehicle groups, indicating that shunt flow induced increased expression of IL-6 and TNFα. Fewer positive signals for IL-6 and TNFα were detected in the EP-NP group, and there was no significant difference in the semiquantitative analysis of IL-6 and TNFα in the EP-NP group compared with the normal group (Figure 4B and C). This suggests that intratracheal instillation of EP-NPs, but not of EP alone or of the vehicle, significantly attenuated increases in IL-6 and TNFα during PAH progression in rats.

Western blot demonstrated that hyperkinetic PAH induced by shunt flow was associated with increased levels of HMGB1 and ET1 in the lung, as confirmed by the bold stripes seen in the blank, EP-only, and vehicle groups (Figure 5A). There was a significant difference in the relative intensity of HMGB1 and ET1 expression between the EP-NP group and the three groups just mentioned ($P<0.05$), but not compared with the normal control group (Figure 5B and C). This suggests that EP-NP intratracheal instillation, but not EP alone or vehicle treatment, was able to reduce the levels of HMGB1 and ET1 in PAH lungs.

EP-NP intratracheal instillation attenuated ROS levels in the lungs

ROS levels were detected under fluorescence microscopy after incubation with DHE (Figure 6A). DHE as an ROS probe was represented by ethidium, which was stained with red fluorescence. Positive signals with less intense red fluorescence were seen in the normal and EP-NP groups, while

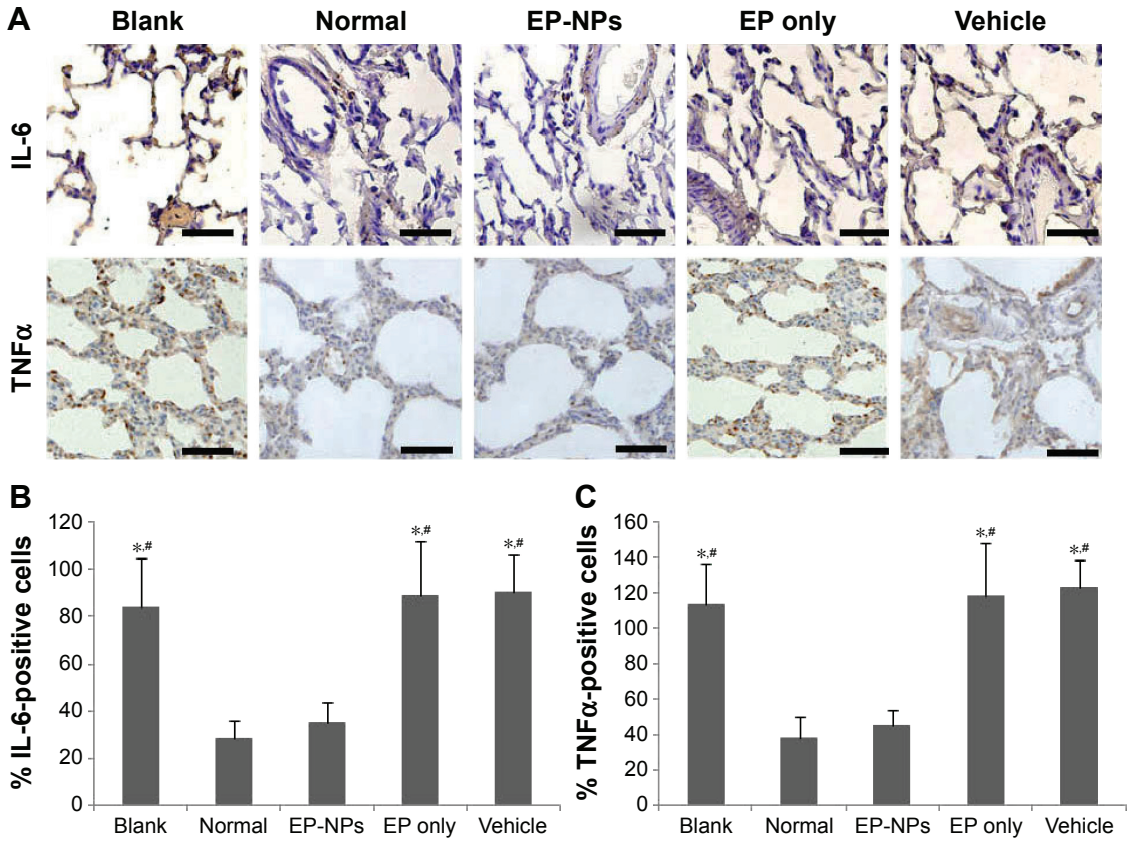

Figure 4 Expression of IL-6 and TNFα in lung tissue.

Notes: (**A**) Representative immunohistochemistry micrographs of IL-6 and TNFα in the different groups. Scale bars 50 μm. (**B**, **C**) Semiquantitative analysis of the immunohistochemistry examination of IL-6 and TNFα (n=100 sections in each group). *$P<0.05$ versus the normal control group; #$P<0.05$ versus the EP-NP group.

Abbreviations: EP-NPs, ethyl pyruvate nanoparticles; EP, ethyl pyruvate.

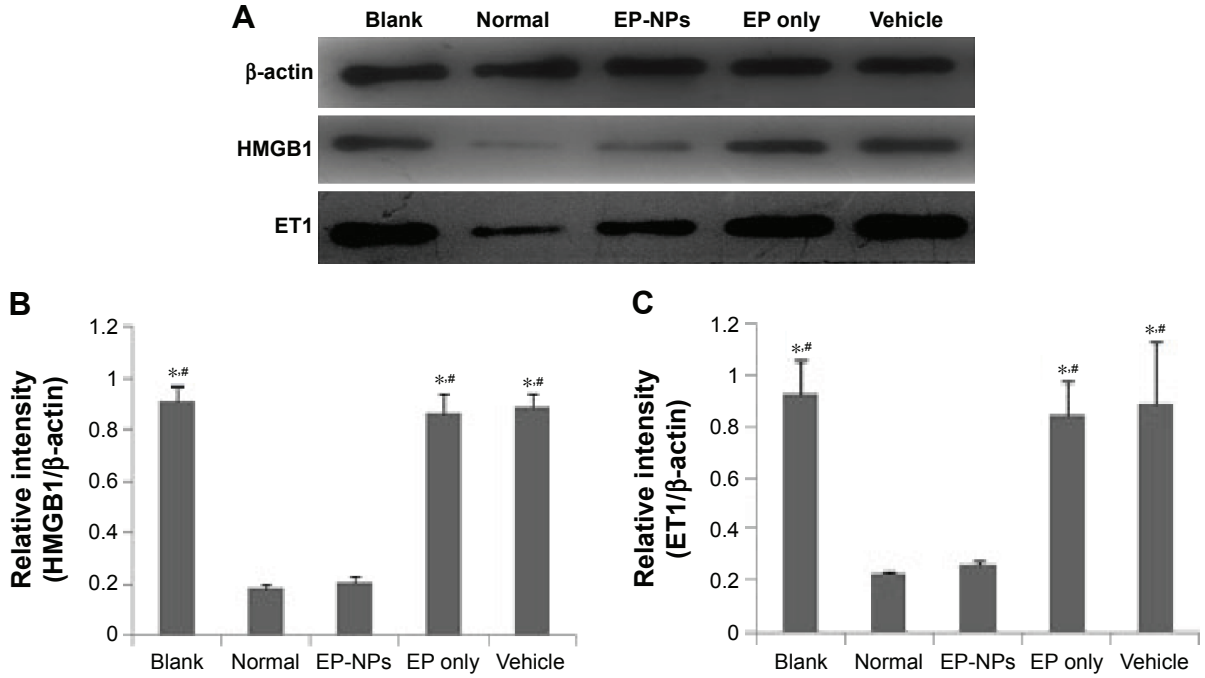

Figure 5 Protein levels of HMGB1 and ET1 in lung tissue.
Notes: (**A**) Expression levels of HMGB1 and ET1 in the lungs were determined using Western blot. (**B**, **C**) Relative intensity of HMGB1 and ET1 in the different groups (n=20 in each group). *$P<0.05$ versus the normal control group; #$P<0.05$ versus the EP-NP group.
Abbreviations: EP-NPs, ethyl pyruvate nanoparticles; EP, ethyl pyruvate.

more intense red fluorescence was seen in the other groups. Ethidium fluorescence-intensity analysis showed decreased ROS content in the EP-NP group compared with the blank, EP-only, and vehicle groups ($P<0.05$, Figure 6B). ROS production in lung homogenates was also measured using another ROS probe: the DCFH-DA fluorescent probe. Fluorescence was similar in the EP-NP and normal control groups, but increased in the blank, vehicle, and EP-only groups (Figure 6C). MDA assay showed that the EP-NP treatment obviously prevented the increased MDA induced by shunt flow compared with the blank, vehicle, and EP-only groups ($P<0.05$, Figure 6D). These ROS-assay results suggest that shunt flow induced elevated ROS levels in the lung, and that EP-NPs, but not EP alone or vehicle instillation, decreased ROS levels in the rat lung tissues.

EP-NP intratracheal instillation decreased the expression of proinflammatory factors and ET1 in serum

ELISA analysis demonstrated that compared with the normal group, significantly increased levels of TNFα, IL-6, HMGB1, and ET1 were seen in the serum of the blank, EP-only, and vehicle groups ($P<0.05$). Serum levels of these proinflammatory factors and ET1 were obviously decreased in the EP-NP group compared with the other treatment groups ($P<0.05$). There were no significant differences in these inflammatory mediators or ET1 between the EP-NP group and the normal group (Figure 7).

EP retention in tissues and plasma

HPLC showed that at the end of the experiment, the lung EP content was significantly higher in the EP-NP group than in the EP-only group ($P<0.05$, Figure 8A). The residual EP content in the other groups was below the limit of detection (data not shown). In the EP-NP group, the EP concentration was lower in other organs (ie, heart, liver, kidney, and spleen) than in the lung tissues. Apart from in the heart, the EP content of the other organs was slightly higher in the EP-NP group than in the EP-only group, but the difference was not significant.

We also measured the EP levels in the lung at different time points after a single instillation of EP-NPs. The lung EP content remained high for the first 3 hours after EP-NP inhalation, followed by a relatively sharp decline in the EP-retention curve 3–12 hours after administration. The level then remained stable until 96 hours, before gradually declining again (Figure 8B). In the EP-only group, the EP content in the lung remained at a low level for the first 2 days, and was thereafter below the limit of detection by HPLC measurement. The serum EP concentration showed a

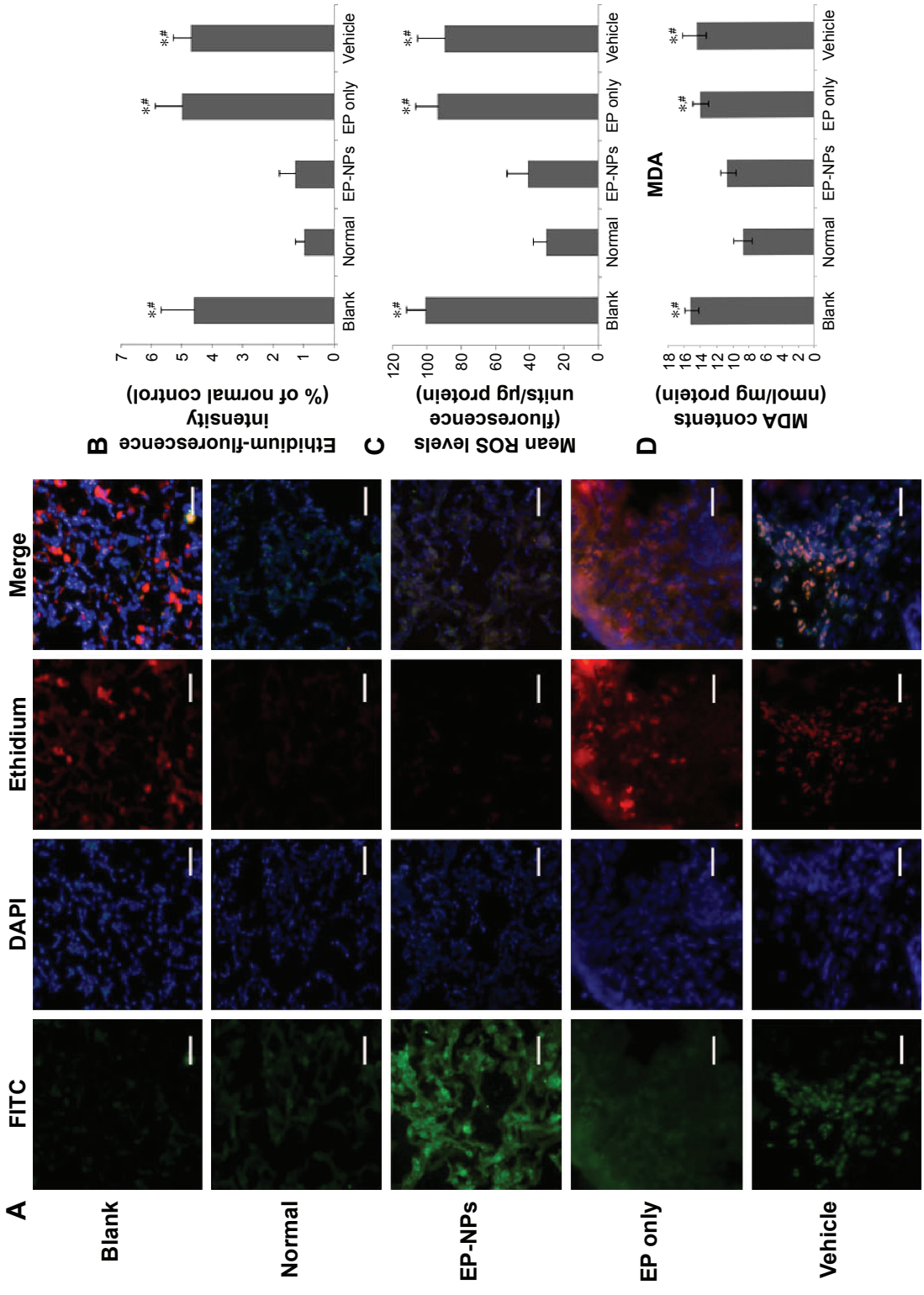

Figure 6 Reactive oxygen species (ROS) assays of the different groups using various methods.

Notes: (**A**) Representative micrographs of ROS levels under a fluorescence microscope after incubation with DHE. FITC indicates the EP-NPs or vehicle location in the lung tissue. DHE as an ROS detector was represented by ethidium, which was stained with red fluorescence in lung sections. Scale bars 30 μm. (**B**) Mean fluorescence of ethidium in the different groups (n=100 sections in each group). Ethidium fluorescence is expressed as a percentage of the normal control (set to 100%). *$P<0.05$ versus the normal control group; #$P<0.05$ versus the EP-NP group. (**C**) ROS production measured in lung homogenates using the DCFH-DA fluorescent probe (n=20 in each group). ROS production is presented as fluorescence units per microgram protein. *$P<0.05$ versus the normal control group; #$P<0.05$ versus the EP-NP group. (**D**) MDA-activity assay in the lung homogenates (n=20 in each group). MDA contents are expressed as nanomoles per milligram protein. *$P<0.05$ versus the normal control group; #$P<0.05$ versus the EP-NP group.

Abbreviations: FITC, fluorescein isothiocyanate; DAPI, 4′,6-diamidino-2-phenylindole; EP-NPs, ethyl pyruvate nanoparticles; DCFH-DA, dichlorofluorescein diacetate; MDA, malondialdehyde; DHE, dihydroethidium; EP, ethyl pyruvate.

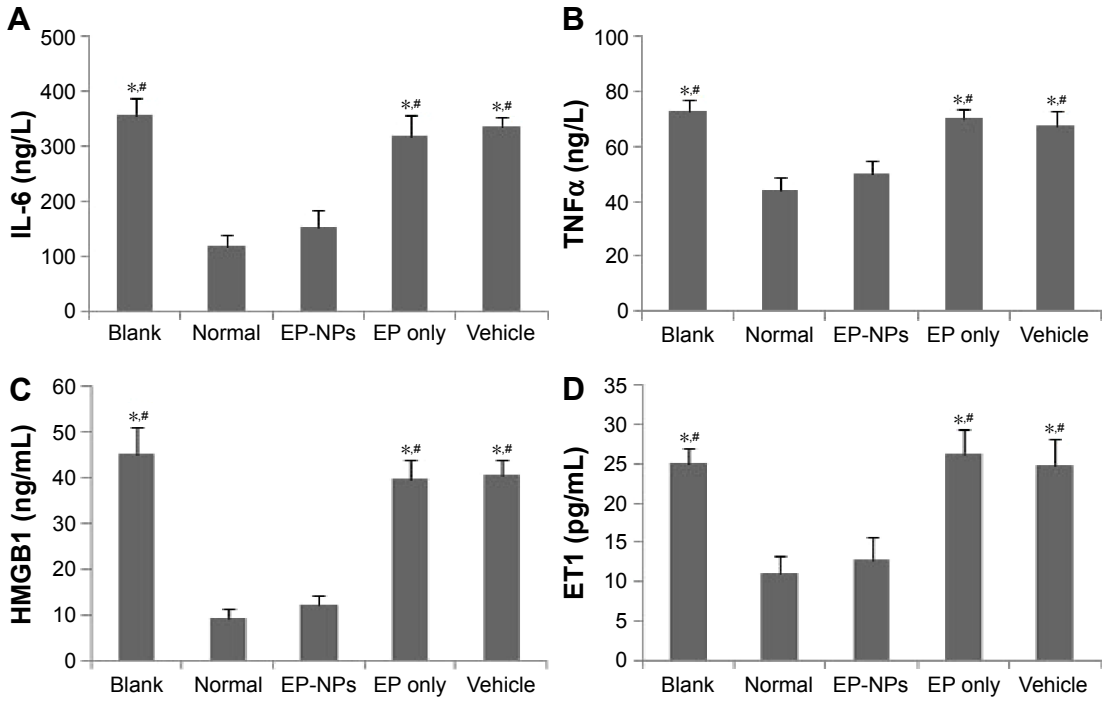

Figure 7 Levels of inflammatory factors and ET1 in serum measured by enzyme-linked immunosorbent assay.
Notes: (**A**–**D**) Levels of IL-6, TNFα, HMGB1, and ET1 in the plasma of the different groups, respectively (n=20 in each group). *$P<0.05$ versus the normal control group; #$P<0.05$ versus the EP-NP group.
Abbreviations: EP-NPs, ethyl pyruvate nanoparticles; EP, ethyl pyruvate.

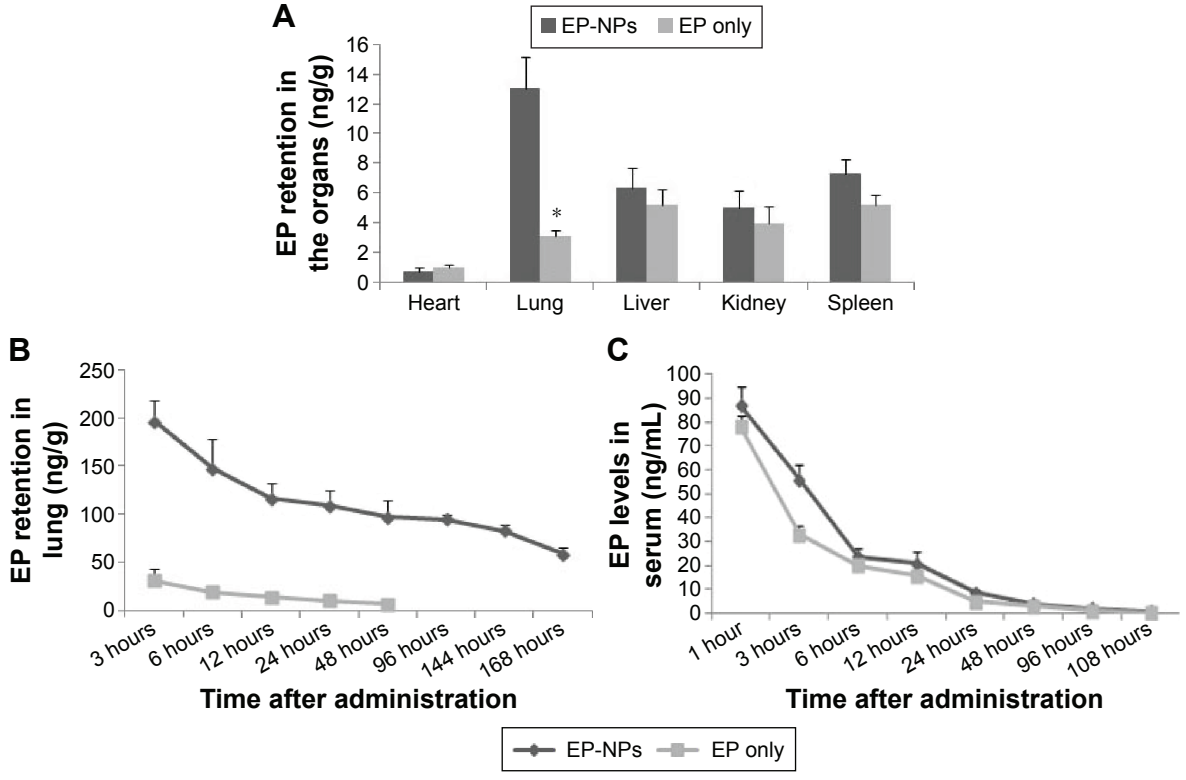

Figure 8 Levels of EP in the organs and serum of the EP-NP and EP-only groups.
Notes: (**A**) EP retention in the organs of the EP-NP and EP-only groups at the end of the experiment (n=20 in each group). *$P<0.05$ versus the EP-NP group. (**B**) Lung EP levels at different time points after a single instillation of EP-NPs or EP (n=5 in each group). (**C**) Serum EP levels at different time points after a single instillation of EP-NPs or EP (n=5 in each group).
Abbreviations: EP-NPs, ethyl pyruvate nanoparticles; EP, ethyl pyruvate.

similar pattern in both the EP-NP and EP-alone groups, with a sharp decreasing trend in the first 6 hours and then low levels until 48 hours; no serum EP was able to be detected after 108 hours (Figure 8C).

Discussion

In this study, we have demonstrated for the first time that EP-NP intratracheal instillation prevents the development of shunt-flow-induced PAH in rats by inhibiting proinflammatory factors and ET1. The following evidence supports our conclusions: 1) intratracheal instilled EP-NPs combined with FITC were observed in the lung tissues, and EP retention was detected after administration; 2) decreased pulmonary circulation resistance, reversed remodeling of the arteries, and hemodynamic improvements were observed after EP-NP inhalation; and 3) the proinflammatory factors IL-6, TNFα, HMGB1, and ROS, as well as ET1, were decreased in the lung after EP-NP instillation during the development of PAH.

It is known that abnormal metabolism is involved in PAH, particularly in RV hypertrophy and remodeling of the pulmonary vasculature. TNFα-mediated inhibition of the metabolic enzyme PDH contributes to the pathogenesis of PAH.[27] Inhibition of PDH induces aerobic glycolysis in both the lungs and the RV, and the glycolytic shift results in decreased contractility of the heart and hyperproliferative endothelial cells.[28] Upregulation of PDH kinase inhibits the activity of PDH and decreases glucose oxidation, whereas inhibition of PDH kinase improves the impaired cardiac function in PAH.[29] EP is a stable aliphatic ester derived from pyruvate. It enters cells freely without the help of a carrier, and is transformed into pyruvate after deesterification.[30] In this study, the antioxidative, anti-inflammatory, and metabolic regulatory functions of EP were found to guarantee its protective effects in the development of PAH. Our results are consistent with those of others, which reported that EP could decrease pulmonary vasoconstriction and downregulate pulmonary artery proinflammatory cytokine gene expression.[16,31] Our previous study described the effects of EP through intraperitoneal injection on monocrotaline-induced PAH.[16] In the current study, however, EP-only intratracheal instillation did not show any therapeutic effects on PAH. This might have been due to the different route of administration, and more importantly because the intraperitoneal injection dose was much higher than that used with intratracheal instillation.

The results from the blank and vehicle groups showed that ET1 and ROS expressions increased during the process of PAH. As we all know, ET1 is one of the most potent vasoconstrictor mediators in promoting endothelial proliferation and fibrosis and reducing the pulmonary vascular bed in PAH. In addition, increased oxidative stress plays an important role in vascular remodeling in PAH in shunted lambs.[32] ET1 activation of ET_A receptors activates the formation of ROS; conversely, ROS can increase ET1-promoter activity and upregulate cellular levels of ET1. In other words, a positive-feedback loop exists between ET1 and ROS production. It has previously been reported that antioxidant treatment of shunted lambs restored unbalanced endothelial function, and some antioxidants have been used in Phase I clinical trials with PAH patients to abrogate ROS generation.[33–35] In the current study, EP-NPs, as powerful ROS scavengers, not only attenuated ROS generation but also decreased ET1 levels during the development of PAH, contributing to its protective effect against PAH.

HMGB1 localizes to the nucleus under normal conditions, and is released to the extracellular milieu in response to injury and inflammatory stimuli.[12] The current study suggests that pulmonary vascular damage in PAH induced by shunt flow triggers the release of a series of inflammatory mediators, including HMGB1, IL-6, TNFα, and ROS. HMGB1 mediates inflammation by binding to cellular receptors such as RAGE, TLR2, and TLR4.[36,37] The major limitation of this study is that the HMGB1 level in bronchoalveolar lavage fluid should be measured in order to investigate the effect of EP-NPs on the release of HMGB1. Previous studies have shown ET1 release to be upregulated in pulmonary arterial endothelial cells by HMGB1 treatment in a dose-dependent manner, and this HMGB1-stimulated increase in ET1 could be inhibited by antibodies against either HMGB1 or RAGE.[4,12] These data demonstrated that HMGB1 induces ET1 release from pulmonary arterial endothelial cells via a RAGE-mediated mechanism. In addition, HMGB1 itself is also involved in vascular remodeling by mediating the proliferation and migration of smooth-muscle cells and endothelial cells.[38,39] EP-NPs act as a potent inflammatory suppressor and HMGB1 inhibitor. In the current study, intratracheal instillation of EP-NPs significantly improved hemodynamic parameters and pulmonary vascular remodeling in PAH rats, possibly as a result of decreased inflammatory mediators and ET1 after EP-NP instillation.

We found EP encapsulated with PEG-LG to be a good drug-delivery system for EP inhalation targeted into the lung. This is supported by the FITC signals, which were not only detected in small bronchial tracts but also around alveolar and small pulmonary arteries within 7 days after a single instillation. The size of drug particles and the aerodynamic

diameters of inhalation particles determine the retention site in the respiratory tract. Particles will be eliminated by expiratory air if the inhalational particles are smaller than 0.5 μm. If the formulation size is larger than 5 μm, however, then particles are deposited in the oropharyngeal area or scavenged by the respiratory cilia. We believe that the faint fluorescence observed in the lung after instillation of FITC alone might be the result of its bigger size. Likewise, in the EP-alone group, most particles might have deposited in the oropharyngeal area or in the upper respiratory tract and have had little impact on the lung. The EP encapsulated with PEG-LG had the optimal particle size and aerodynamic diameter for inhalation, which guaranteed it would act at the correct site in the lung. HPLC showed that EP-NPs were released in a slow, easily controlled, and targeted manner. Therefore, this formulation enhanced the bioavailability of EP, improved its stability, and reduced or avoided the adverse effects that can be induced by systemic administration. The advantages of NP-mediated drug-delivery systems for the treatment of lung diseases, including PAH, have also been confirmed in other studies.[40,41]

According to our prior experiment, the in vitro release profile of EP-NPs showed sustained release of 85% EP for at least 168 hours, with a small burst release. In the current in vivo experiments, fluorescence was faint 7 days after FITC-NP administration (Figure 2). Therefore, EP-NPs were administered weekly in the current study. HPLC also confirmed that this frequency of treatment was reasonable. At the end of the experiment, far more EP was retained in the lungs in the EP-NP group than in other organs, which is characteristic of intratracheal drug delivery. Although serum EP retention was similar in the EP-NP and EP-only groups before 48 hours, plasma levels of inflammatory mediators and ET1 were lower in the EP-NP group. We think that during the first 6 hours after inhalation, the EP plasma concentration was high enough to suppress inflammation to some degree in both groups. Six hours later, however, the drug levels were too low to restrain inflammatory mediators. Moreover, overflow and high pressure in the lung induced persistent release of inflammatory factors into the circulation. Under these circumstances, inflammation could not be suppressed in the EP-only group. In the EP-NP group, however, the high retention of EP in the lung not only inhibited pulmonary inflammation but also attenuated the release of inflammatory factors into the circulation.

We observed no toxicologic or other adverse reactions caused by the EP-NP inhalation-delivery system in rats over 12 weeks. This indicates that the polymeric materials used to fabricate the particles are safe for relatively long-term administration. This agrees with a previous study, in which a lactide/glycolide copolymer (PLGA) used as a carrier for intratracheal instillation for 21 days resulted in no toxicologic reactions.[41] Nonetheless, the long-term safety and therapeutic effects of an NP-mediated EP system in PAH should be explored in further studies. In addition, the accumulation or clearance rate of polymeric materials from the lungs over time should be taken into account in providing more information about the use of such a system.

Conclusion

NP-mediated delivery of EP into the lung had a protective effect against the progression of PAH induced by shunt flow in rats. EP-NP instillation improved hemodynamics in rats and vascular remodeling by suppressing inflammatory mediators and ET1 in the development of PAH. EP-NPs show promise as a potential antioxidant for preventing the disease process in PAH patients.

Acknowledgments

We sincerely thank Xuping Wang for assistance in immunofluorescence examination. We also thank Shanying Huang (pathologist) for providing kind instructions on histological analysis. This study was supported by a grant (BS2013YY016) from the Doctor Foundation of Shandong Province, PRC.

Disclosure

The authors report no conflicts of interest in this work.

References

1. Voelkel NF, Quaife RA, Leinwand LA, et al. Right ventricular function and failure: report of a National Heart, Lung, and Blood Institute working group on cellular and molecular mechanisms of right heart failure. *Circulation*. 2006;114(17):1883–1891.
2. Li W, Sama AE, Wang HC. Role of HMGB1 in cardiovascular diseases. *Curr Opin Pharmacol*. 2006;6(2):130–135.
3. Sadamura-Takenaka Y, Ito T, Noma S, et al. HMGB1 promotes the development of pulmonary arterial hypertension in rats. *PLoS One*. 2014;9(7):e102482.
4. Bauer EM, Shapiro R, Zheng H, et al. High mobility group box 1 contributes to the pathogenesis of experimental pulmonary hypertension via activation of Toll-like receptor 4. *Mol Med*. 2012;18:1509–1518.
5. Price LC, Wort SJ, Perros F, et al. Inflammation in pulmonary arterial hypertension. *Chest*. 2012;141(1):210–221.
6. Tuder RM, Archer SL, Dorfmüller P, et al. Relevant issues in the pathology and pathobiology of pulmonary hypertension. *J Am Coll Cardiol*. 2013;62(25 Suppl):D4–D12.
7. Groth A, Vrugt B, Brock M, Speich R, Ulrich S, Huber LC. Inflammatory cytokines in pulmonary hypertension. *Respir Res*. 2014;15(1):47–57.
8. Hassoun PM. Inflammation in pulmonary arterial hypertension: is it time to quell the fire? *Eur Respir J*. 2014;43(3):685–688.

9. Brock M, Trenkmann M, Gay RE, et al. Interleukin-6 modulates the expression of the bone morphogenic protein receptor type ii through a novel stat3-microRNA cluster 17/92 pathway. *Circ Res*. 2009;104(10):1184–1191.
10. Firth AL, Yuill KH, Smirnov SV. Mitochondria-dependent regulation of Kv currents in rat pulmonary artery smooth muscle cells. *Am J Physiol Lung Cell Mol Physiol*. 2008;295(1):L61–L70.
11. Hu HL, Zhang ZX, Chen CS, Cai C, Zhao JP, Wang XD. Effects of mitochondrial potassium channel and membrane potential on hypoxic human pulmonary artery smooth muscle cells. *Am J Respir Cell Mol Biol*. 2010;42(6):661–666.
12. Yang PS, Kim DH, Lee YJ, et al. Glycyrrhizin, inhibitor of high mobility group box-1, attenuates monocrotaline-induced pulmonary hypertension and vascular remodeling in rats. *Respir Res*. 2014;15(1):148.
13. Kao KK, Fink MP. The biochemical basis for the anti-inflammatory cytoprotective actions of ethyl pyruvate and related compounds. *Biochem Pharmacol*. 2010;80(2):151–159.
14. Fink MP. Ethyl pyruvate: a novel anti-inflammatory agent. *J Intern Med*. 2007;261(4):349–362.
15. Matone J, Moretti AI, Apodaca-Torrez FR, Goldenberg A. Ethyl-pyruvate reduces lung injury matrix metalloproteinases and cytokines and improves survival in experimental model of severe acute pancreatitis. *Acta Cir Bras*. 2013;28(8):559–567.
16. Liu C, Fang C, Cao G, et al. Ethyl pyruvate ameliorates monocrotaline-induced pulmonary arterial hypertension in rats. *J Cardiovasc Pharmacol*. 2014;6(1):7–15.
17. Kawashima Y, Yamamoto H, Takeuchi H, Hino T, Niwa T. Properties of a peptide containing DL-lactide/glycolide copolymer nanospheres prepared by novel emulsion solvent diffusion methods. *Eur J Pharm Biopharm*. 1998;45(1):41–48.
18. Kawashima Y, Yamamoto H, Takeuchi H, Fujioka S, Hino T. Pulmonary delivery of insulin with nebulized DL-lactide/glycolide copolymer (LG) nanospheres to prolong hypoglycemic effect. *J Control Release*. 1999;62(1–2):279–287.
19. Liu K, Liu R, Cao G, Sun H, Wang X, Wu S. Adipose-derived stromal cell autologous transplantation ameliorates pulmonary arterial hypertension induced by shunt flow in rat models. *Stem Cells Dev*. 2011;20(6):1001–1010.
20. Everett AD, Le Cras TD, Xue C, Johns RA. eNOS expression is not altered in pulmonary vascular remodeling due to increased pulmonary blood flow. *Am J Physiol*. 1998;274(6 Pt 1):L1058–L1065.
21. Megalou AJ, Glava C, Oikonomidis DL, et al. Transforming growth factor-β inhibition attenuates pulmonary arterial hypertension in rats. *Int J Clin Exp Med*. 2010;3(4):332–340.
22. Miller FJ Jr, Gutterman DD, Rios CD, Heistad DD, Davidson BL. Superoxide production in vascular smooth muscle contributes to oxidative stress and impaired relaxation in atherosclerosis. *Circ Res*. 1998;82(12):1298–1305.
23. Wang XP, Chen YG, Qin WD, et al. Arginase I attenuate inflammatory cytokine secretion induced by lipopolysaccharide in vascular smooth muscle cells. *Arterioscler Thromb Vasc Biol*. 2011;31(8):1853–1860.
24. Bejma J, Ramires P, Ji LL. Free radical generation and oxidative stress with ageing and exercise: differential effects in the myocardium and liver. *Acta Physiol Scand*. 2000;169(4):343–351.
25. Lebel CP, Bondy SC. Sensitive and rapid quantitation of oxygen reactive species formation in rat synaptosomes. *Neurochem Int*. 1990;17(3):435–440.
26. Liu K, Cao G, Zhang X, Liu R, Zou W, Wu S. Pretreatment with intraluminal rapamycin nanoparticle perfusion inhibits neointimal hyperplasia in a rabbit vein graft model. *Int J Nanomedicine*. 2010;5:853–860.
27. Sutendra G, Dromparis P, Bonnet S, et al. Pyruvate dehydrogenase inhibition by the inflammatory cytokine TNFα contributes to the pathogenesis of pulmonary arterial hypertension. *J Mol Med (Berl)*. 2011;89(8):771–783.
28. Archer SL, Fang YH, Ryan JJ, Piao L. Metabolism and bioenergetics in the right ventricle and pulmonary vasculature in pulmonary hypertension. *Pulm Circ*. 2013;3(1):144–152.
29. Piao L, Sidhu VK, Fang YH, et al. FOXO1-mediated upregulation of pyruvate dehydrogenase kinase-4 (PDK4) decreases glucose oxidation and impairs right ventricular function in pulmonary hypertension: therapeutic benefits of dichloroacetate. *J Mol Med (Berl)*. 2013;91(3):333–346.
30. Kim JB, Yu YM, Kim SW, Lee JK. Anti-inflammatory mechanism is involved in ethyl pyruvate-mediated efficacious neuroprotection in the postischemic brain. *Brain Res*. 2005;1060(1–2):188–192.
31. Tsai BM, Lahm T, Morrell ED, et al. Ethyl pyruvate inhibits hypoxic pulmonary vasoconstriction and attenuates pulmonary artery cytokine expression. *J Surg Res*. 2008;145(1):130–134.
32. Grobe AC, Wells SM, Benavidez E, et al. Increased oxidative stress in lambs with increased pulmonary blood flow and pulmonary hypertension: role of NADPH oxidase and endothelial NO synthase. *Am J Physiol Lung Cell Mol Physiol*. 2006;290(6):L1069–L1077.
33. Steinhorn RH, Albert G, Swartz DD, Russell JA, Levine CR, Davis JM. Recombinant human superoxide dismutase enhances the effect of inhaled nitric oxide in persistent pulmonary hypertension. *Am J Respir Crit Care Med*. 2001;164(5):834–839.
34. McMurtry MS, Bonnet S, Wu X, et al. Dichloroacetate prevents and reverses pulmonary hypertension by inducing pulmonary artery smooth muscle cell apoptosis. *Circ Res*. 2004;95(8):830–840.
35. Rosenfeldt FL, Haas SJ, Krum H, et al. Coenzyme Q_{10} in the treatment of hypertension: a meta-analysis of the clinical trials. *J Hum Hypertens*. 2007;21(4):297–306.
36. van Zoelen MA, Yang H, Florquin S, et al. Role of Toll-like receptors 2 and 4, and the receptor for advanced glycation end products in high-mobility group box 1-induced inflammation in vivo. *Shock*. 2009;31(3):280–284.
37. van Beijnum JR, Buurman WA, Griffioen AW, et al. Convergence and amplification of Toll-like receptor (TLR) and receptor for advanced glycation end products (RAGE) signaling pathways via high mobility group B1 (HMGB1). *Angiogenesis*. 2008;11(1):91–99.
38. Treutiger CJ, Mullins GE, Johansson AS, et al. High mobility group 1 B-box mediates activation of human endothelium. *J Intern Med*. 2003;254(4):375–385.
39. Fiuza C, Bustin M, Talwar S, et al. Inflammation-promoting activity of HMGB1 on human microvascular endothelial cells. *Blood*. 2003;101(1):2652–2660.
40. Kimura S, Egashira K, Chen L, et al. Nanoparticle-mediated delivery of nuclear factor κB decoy into lungs ameliorates monocrotaline-induced pulmonary arterial hypertension. *Hypertension*. 2009;53(5):877–883.
41. Chen L, Nakano K, Kimura S, et al. Nanoparticle-mediated delivery of pitavastatin into lungs ameliorates the development and induces regression of monocrotaline-induced pulmonary artery hypertension. *Hypertension*. 2011;57(2):343–350.